Dalton Transactions

PAPER

View Article Online
View Journal | View Issue

Cite this: *Dalton Trans.*, 2018, **47**, 16145

Selective signalling of glyphosate in water using europium luminescence†‡

Laura B. Jennings, Sergey Shuvaev, Mark A. Fox, Robert Pal and David Parker *

Received 21st September 2018,
Accepted 23rd October 2018

DOI: 10.1039/c8dt03823f

rsc.li/dalton

A series of four emissive europium complexes has been evaluated for the binding of glyphosate in various aqueous media, including river water and grain extracts. Binding selectivity toward inorganic phosphate and bicarbonate was enhanced by measuring samples at pH 5.9, above the pK_a of glyphosate itself. The highest affinity was shown with [Eu·L[1]], which creates an exocyclic tripicolylamine moiety when one pyridine group dissociates from Eu. Glyphosate was bound selectively over dihydrogenphosphate, glycinate, aminomethylphosphonate and the related herbicide glufosinate. The complex was used to measure glyphosate over the range 5 to 50 μM, in river water and grain extracts.

Introduction

Glyphosate (*N*-(phosphonomethyl)glycine), **1** is a broad-spectrum, post-emergence, systemic herbicide that became popular because of the demands of intensive farming. It was discovered by Monsanto in the early 1970s, and is the active ingredient in 'Roundup' and many weed-killers.[1] It has become the most widely used herbicide by volume, being manufactured and sold by various companies around the globe.[2] The popularity of glyphosate was firmly established as Monsanto developed 'Roundup Ready' crops, such as cotton, corn and soya-bean, that are resistant to the herbicide and are widely grown.[3]

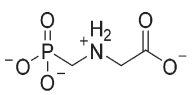

1

However, over the past few years increasing concerns about the safety of the chemical has led to a thorough investigation of its carcinogenicity.[4] Initially, it was considered to be one of the safest herbicides in existence, as it works through disruption of the shikimate biosynthetic pathway that does not exist in mammals.[5,6] Specifically, glyphosate is absorbed through the foliage and minimally through the roots, where it migrates to the plant tips. Here, it inhibits the enzyme EPSP-synthase, which is necessary for growth; EPSP-synthase catalyses the reaction between shikimate-3-phosphate and phosphoenolpyruvate, to form 5-enolpyruvylshikimate-3-phosphate (EPSP). The reaction is a key part of the shikimate pathway, in which the aromatic amino acids phenylalanine, tryptophan and tyrosine are biosynthesised;[7] without these essential amino acids, the plant cannot survive.

Limits on the presence of glyphosate in food and water have been set by a number of agencies around the world. It is generally considered that current levels in water are well below dangerous concentrations. Indeed, neither the WHO, the EU, nor the UK regulatory authorities have set an MRL (minimal residual level). However, the US EPA set a limit of 0.7 mg L^{-1} (4.1×10^{-6} M) as a precaution, although levels this high have never been detected in drinking water.[8] Glyphosate has also been found to decompose rapidly in chlorinated water and so it is unlikely that large concentrations will be found in tap water.[9] It is accepted that the main source of glyphosate for the general populous is through diet, so that most foods have a safety limit at a much lower concentration. At such levels, it is generally accepted that there is a minimal risk to cause cancer.[10] Limits have been set by a number of organisations across the world.[11–13] Grain, fruit and vegetables have all been given MRLs, to ensure that the level of glyphosate consumed is well below 'dangerous levels'.

Studies of glyphosate recognition in aqueous solution using designed synthetic receptors are rare. Protonated polyamines[14] or PAMAM dendrimers[15] linked or including an aromatic fluorophore have been shown to bind the anion electrostatically, but without any significant chemoselectivity. The latter example was based on the idea of competitive fluorophore displacement, and more recent examples of this approach have been reported, *e.g.* using a *tris*-thiourea recognition motif,[16] albeit in 95 : 5 DMSO/H_2O. Again, no selectivity of any consequence was found for glyphosate over key

Department of Chemistry, Durham University, South Road, Durham, DH1 3LE, UK. E-mail: david.parker@dur.ac.uk

† Dedicated to Geoff Cloke on the occasion of reaching the age of Wisdom.

‡ Electronic supplementary information (ESI) available. See DOI: 10.1039/c8dt03823f

competing anions, such as inorganic phosphate or hydrogencarbonate.

Our approach to anion recognition in water has used direct metal coordination of the anion to a lanthanide centre, displacing a coordinated water molecule or a weakly bound ligand donor atom, accompanied by stabilising intramolecular hydrogen bonding.[17] The binding process can be monitored and signalled by NMR and emission spectroscopy. During the course of a series of studies examining the recognition of various anions by emissive lanthanide(III) complexes,[18,19] it was discovered that certain nucleotides, notably ADP and ATP, bound reversibly to the complex [EuL^1], and that this reversible binding process could be followed by circular polarized luminescence (CPL) spectroscopy, distinguishing ADP from ATP binding by the sign of the induced CPL signal.[20]

The model used to rationalise this behaviour involves phosphate binding to the Eu ion, following dissociation of the 2,6-disubstituted pyridyl N atom, wherein the ternary adduct is either stabilized by H-bonding to the tertiary aliphatic amine N, or involves phosphate bridging to a bound Zn^{2+} ion (Scheme 1) that displaces the 3° amine proton and occupies the exocyclic poly-aza binding site.

With this background in mind we set out to examine the binding of the complex [HEu·L^1]$^+$ and its structural analogues, [HEu·L^{2-4+}] (Scheme 2), lacking one or two pyridyl groups to glyphosate, **1**, and structurally related congeners, including glycinate, the primary metabolite aminomethylphosphonic acid, **2**, (AMPA, pK_a = 5.36) the *N*-methyl derivative, **3**, and the related herbicide glufosinate, **4** that possesses a methylphosphinate moiety rather than a phosphonate group (Scheme 3).

Binding behaviour was examined in saline solution, in the absence and presence of added zinc ions, and in aqueous samples that are more representative of real-world applications, *e.g.* river water samples or aqueous grain extracts.

Results and discussion

Protonation equilibria

A key to devising chemoselectivity towards glyphosate in water is to consider its protonation equilibria carefully, Scheme 4. Such an approach has not overtly been discussed in enhancing selectivity in aqueous solution. Deprotonation of the phosphate oxygen is associated with a measured pK_a value of 5.57,[21] that was more recently estimated to be 5.69, in zero ionic strength solution.[22] This pK_a value can be compared to those of carbonic acid (6.16) and $H_2PO_4^-$/HPO_4^{2-} (7.21). It was therefore reasoned that selectivity over phosphate and hydrogencarbonate in analysing for glyphosate in water can be created by working at pH 5.9, as it still exists predominantly as a di-anion at this pH, and hence should have a much greater affinity for the cationic Eu(III) centre.

Three of the four europium complexes, [Eu·L$^{1-3}$] have been described earlier,[20] and the pyrazole system, [Eu·L^4] was prepared in an analogous manner (ESI†). Each complex contains sites for protonation at the pyridine/pyrazole N atoms and at the tertiary aliphatic N atom. The europium emission spectral form was found to vary with pH, in a manner that reflects the exquisite sensitivity of the Eu spectral fingerprint to perturbation of the second sphere of coordination and to changes in proximate donor atom polarisabilities.[23,24]

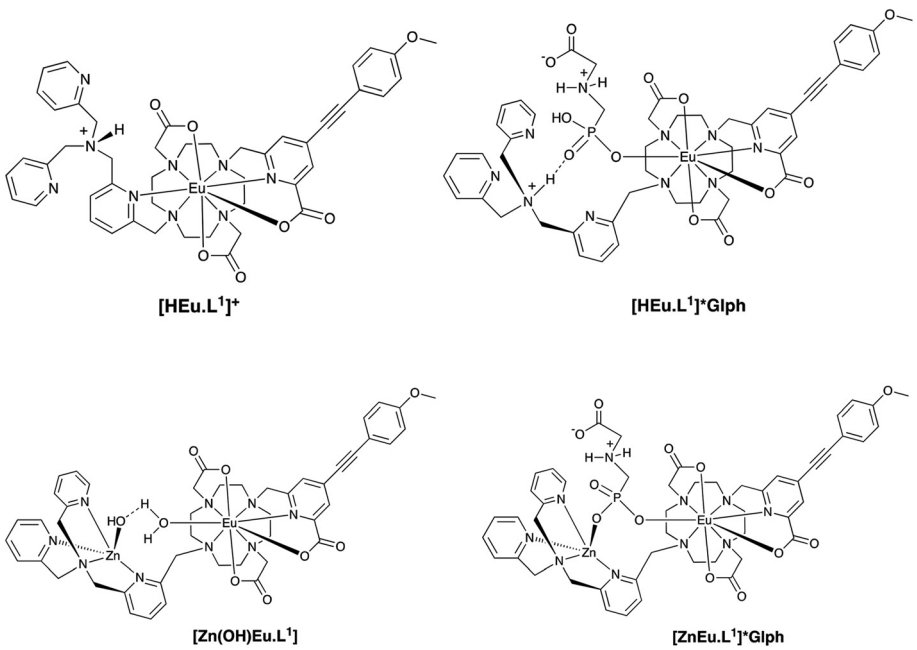

Scheme 1

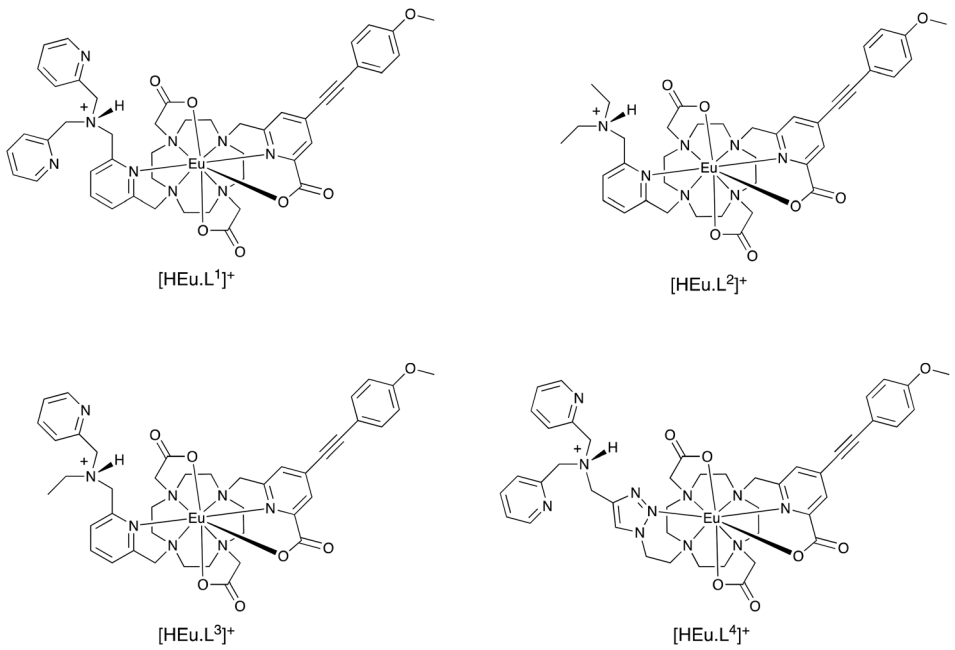

Scheme 2

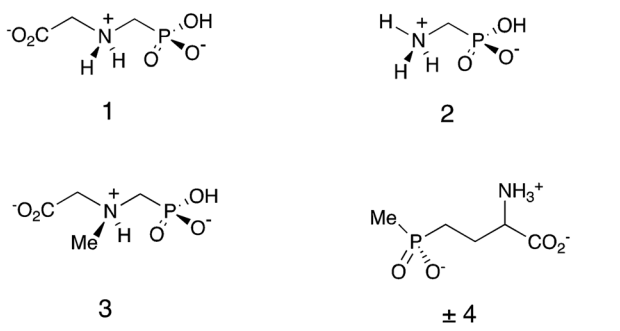

Scheme 3

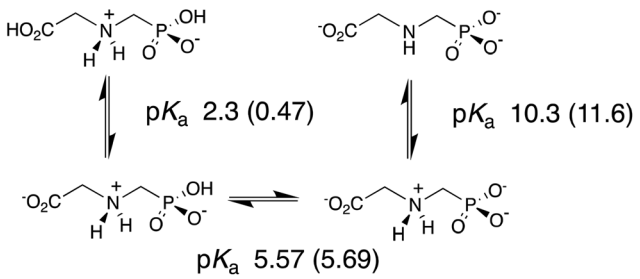

Scheme 4 Experimental[21] (0.1 M NaCl) and, in parentheses, the corresponding calculated[22] (I = 0) pK_a values for glyphosate.

The pK_a values of each of the four the complexes were determined (0.1 M NaCl solution), by following changes in the intensity ratio of pairs of Eu emission bands, as a function of pH (Fig. 1, Table 1 and Fig. S1, S2†).

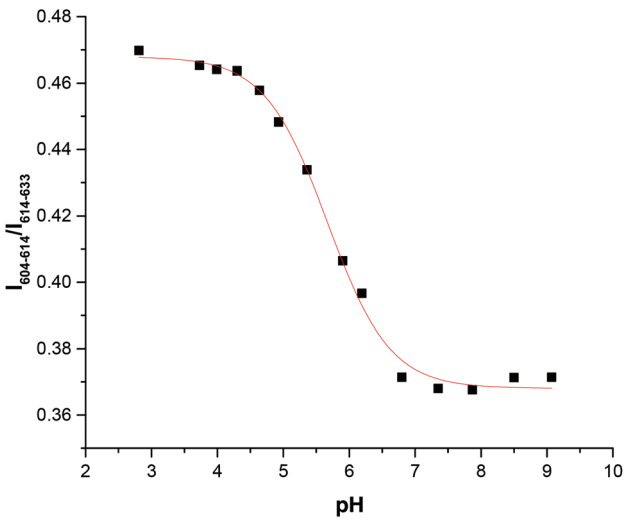

Fig. 1 Variation of the europium emission intensity ratio (604–614 nm/614–633 nm) with pH for [Eu·L^1] ([complex] = 7 μM, 0.1 M NaCl, 295 K, λ_{ex} 340 nm), showing the fit (line) to the experimental data points (Table 1). At higher pH (>11), bicarbonate may bind competitively to the Eu centre, displacing a coordinated pyridine donor.

Table 1 Values of pK_a measured for the complexes, [Eu·L$^{1-4}$] (295 K, 0.1 M NaCl)

Complex	pK_a value
[Eu·L^1]	5.67 (±0.04)
[Eu·L^2]	7.60 (±0.06)
[Eu·L^3]	6.99 (±0.05)
[Eu·L^4]	<2.5

The first pK_a value of [Eu·L^1] was determined to be 5.67 (±0.04) and the complex is substantially deprotonated under the conditions of the analyte titration experiments at pH 5.9. This value may be compared to the pK_a value of 6.17, reported for *tris*(2-methylpyridyl)amine.[25] In [Eu·L^3] and [Eu·L^2], one or two picolyl groups are replaced with ethyl groups, and the pK_a value was raised to 6.99 (±0.05) for [Eu·L^3] and 7.60 (±0.06) for [Eu·L^2]. Hence, the tertiary amine N atom will be 93 and 98% protonated at pH 5.9, respectively, modulating the hydrogen bonding and metal binding capabilities of the complex. The pK_a value for [Eu·L^4] was not determined, despite starting the titration at pH 3.5, in line with the low pK_a value of such triazole compounds.

Computational studies of glyphosate binding

In order to assess the feasibility of cooperative binding interactions that may stabilise the ternary adduct when the phosphate oxygen binds to the Eu ion, a set of DFT computations was undertaken. The model geometries for the putative glyphosate adducts, **[HEuL1]*Glph** and [EuL^1]*Zn^{2+}*Glph, in this work were fully optimised without symmetry constraints, using the hybrid-DFT B3LYP functional[26] and the 3-21G* basis set[27] for all atoms with the Gaussian 09 package.[28] The 4-methoxyphenylethynyl group in ligand L^1 was replaced with a hydrogen atom in the model geometries, to reduce computational efforts. The paramagnetic Eu(III) complexes are difficult to model computationally, so Y(III) has been used instead of Eu(III), as described in calculations elsewhere.[29] Optimised geometries of Y(III) complexes with the B3LYP/3-21G* functional/basis set have been demonstrated previously to be suitable models for Eu(III) complexes.[17,19] The Gaussian09 default polarisation continuum solvent model (IEFPCM)[30] was applied to all calculations, using water as the solvent.

The optimised model geometry for [EuL^1]*Glph (Fig. 2), revealed phosphate-O to Eu coordination, with cooperative H-bonding involving a strong N–H···O interaction with an H···O distance of 1.47 Å, and two N–H···N interactions with H···N distances of 1.84 and 1.88 Å. In the zinc–bound adduct, the phosphate bridges the two metal ions, and the tertiary amine N is coordinated to the Zn ion.

Complexation behaviour with glyphosate and its congeners

The addition of glyphosate to [Eu·L^1] was monitored by time-gated luminescence spectroscopy with excitation at 365 nm, allowing ten minutes equilibration after addition of each increment. Iterative non-linear least squares fitting of the binding isotherm (Fig. 3) gave an apparent log K value of 5.36 (±0.02). A significant change in the emission spectral form and relative band intensities occurred after addition of glyphosate, notably in the magnetic-dipole allowed $\Delta J = 1$ transitions around 590 nm and in the hypersensitive $\Delta J = 2$ manifold. Such behaviour was similar in nature to that observed earlier with ADP or ATP,[20] for which photo-assisted dissociation of the non-conjugated pyridine N was assumed to have occurred, followed by binding of the phosphate oxygen atom to the Eu(III) ion, consistent with the proposed DFT computational structure. The

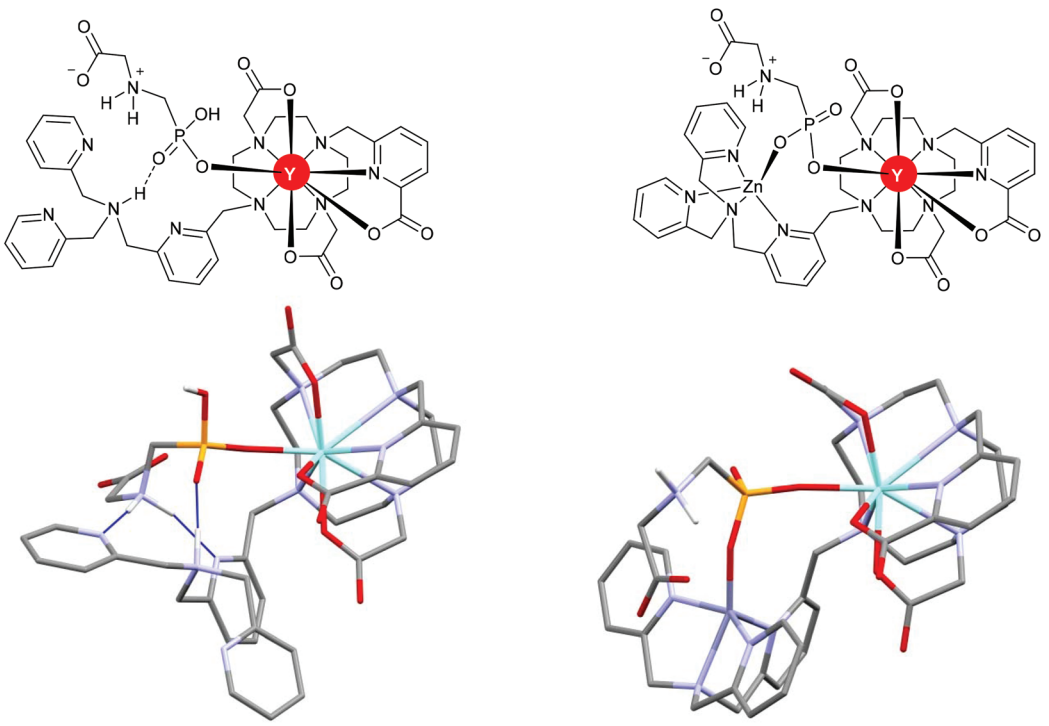

Fig. 2 Optimised model geometries for **[HEuL^1]*Glph** and **[ZnEuL^1]*Glph** adducts, showing hydrogen bonding interactions. Hydrogen atoms bound to carbon are omitted for clarity, and Y is used as a surrogate for the Eu ion. The figures of optimised model geometries were generated using Mercury software.[31]

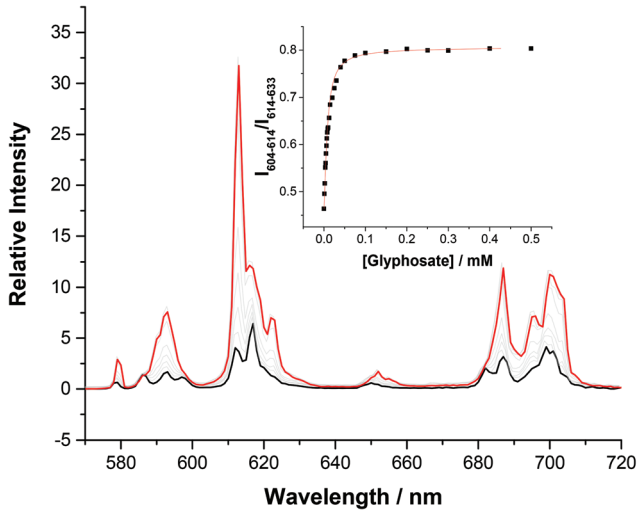

Fig. 3 Changes in the emission intensity of [Eu·L^1] (black) (6 μM complex, 0.1 M NaCl, 0.1 M MES, pH 5.9, 295 K, λ_{ex} 365 nm) with incremental addition of glyphosate (red). The inset shows the variation of the emission intensity ratio (604–614/614–633 nm) as a function of increasing glyphosate concentration, showing the best fit (line) with log K = 5.36 (02).

Table 2 The europium radiative lifetimes, τ, for [Eu·L^1], (7 μM], with and without added glyphosate (10 fold excess) in H_2O and D_2O, with the corresponding values of the hydration number, q.[32]

Complex	τ_{H_2O}/ms	τ_{D_2O}/ms	q (±0.2)
[Eu·L^1]	0.55	0.73	0.2
[Eu·L^1] + glyphosate	0.79	1.36	0.3

linear range of this response lies within the MRL values suggested for glyphosate, suggesting scope for its use as a probe.

The Eu emission lifetimes were recorded at the start and end of each titration in H_2O and D_2O, to allow the hydration number, q, to be calculated (Table 2).[32] In each case, the q value is approximately zero, showing that there is no water in the inner sphere, consistent with a coordination number of nine around the europium(III) ion. Thus, the phosphate oxygen atom displaces the pyridyl nitrogen atom, in the ternary adduct. Similar q values were recorded for the other three Eu complexes studied, under these conditions, and in the presence of added zinc ions for [EuL^1].

No evidence for binding to [Eu·L^1] was observed with glycinate and glufosinate at pH 5.9, and the measured binding constants for dihydrogenphosphate, *N*-methylglyphosate, **3**, and aminomethylphosphonate, AMPA **2**, were log K = 4.35, 3.93 and 3.30 respectively (Fig. S4–S6†). Thus, the binding affinity is between one and two orders of magnitude less strong than with glyphosate itself. Such behaviour presumably reflects both the absence of stabilising directed hydrogen bonding interactions in these adducts (Fig. 1) and the differing free energies of hydration, for the free and bound species. With *N*-methyl glyphosate, the presence of the methyl group may also limit the extent of the hydrogen bonding array (Fig. 2), possibly by a steric effect that suppresses adduct solvation.

Experiments with added zinc ions

Before assessing the glyphosate binding behaviour when zinc ions were also added, control experiments were undertaken with added $ZnCl_2$ alone, using [Eu·L^1] and [Eu·L^2]. Inspection of the binding curve of [EuL^1] with added Zn^{2+} indicated a 1 : 2 binding stoichiometry (Fig. 4), suggesting that the Zn^{2+} ion bridges two europium complexes. This assumption was confirmed by a Job plot (Fig. 5). A high overall binding affinity to Zn^{2+} ions was estimated (log K *ca.* 7.5), accompanied by little overall change in the Eu^{3+} emission lifetime (τ = 0.46 ms), indicating that the metal hydration state did not change However, the binding constant value should be treated with much caution, as it was calculated assuming a limiting 1 : 1 binding model, and is only an approximation.

Similar behaviour was observed with added Ni^{2+}. Addition of a large excess of alkali-earth metal ions, such as Ca^{2+} and Mg^{2+} and transition metal chloride salts, such as Cr^{3+} and Mn^{2+} only slightly changed the total emission intensity, and did not affect the spectral signature.

The complex [EuL^2], where an ethyl group replacing one pyridine showed similar overall binding behaviour. The total emission intensity underwent a significant 10-fold rise, along with a major change in spectral form (Fig. 6); the lifetime of the excited state doubled upon addition of Zn^{2+} rising from 0.22 ms to 0.46 ms. A Job plot suggested that 1 : 1 binding was dominant in this case (Fig S3, ESI†). Indeed, these Eu com-

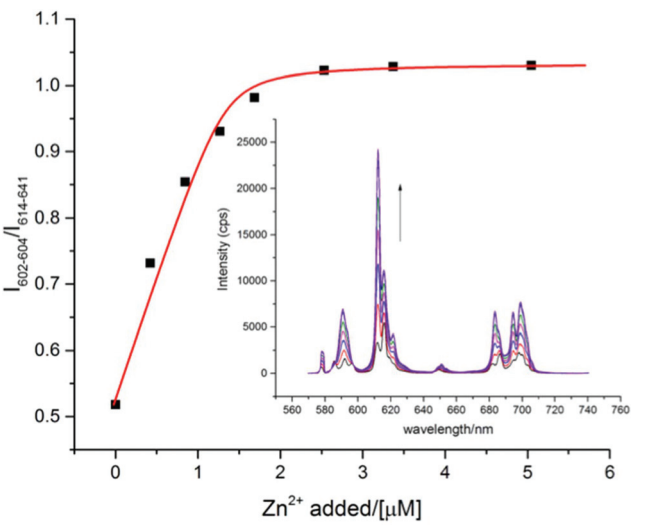

Fig. 4 Variation of the emission intensity ratio and the overall emission spectrum of [EuL^1] (inset) with added $ZnCl_2$ ([EuL^1] 5 μM, 0.1 M HEPES, pH = 7.40, 298 K, λ_{ex} = 335 nm), showing the large change in the form of the ΔJ = 1 manifold around 590 nm, consistent with a large change in the Eu coordination environment The approximate binding affinity (log K = 7.5) was estimated using a simple 1 : 1 binding model.

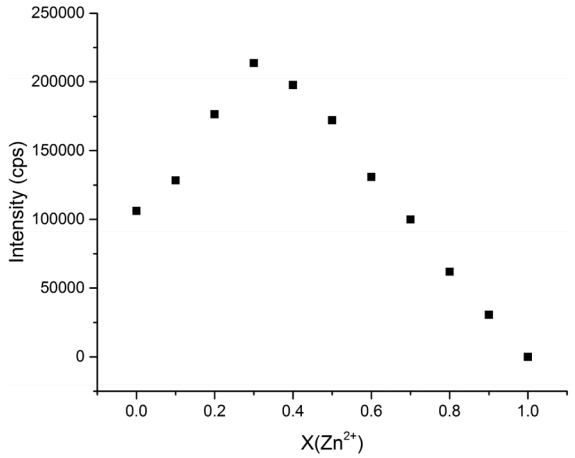

Fig. 5 Job plot for [EuL^1] following the emission intensity change at 616 nm as a function of mole fraction $ZnCl_2$ ([EuL^1] 5 μM, 0.1 M HEPES, pH 7.40, 298 K, λ_{ex} = 335 nm).

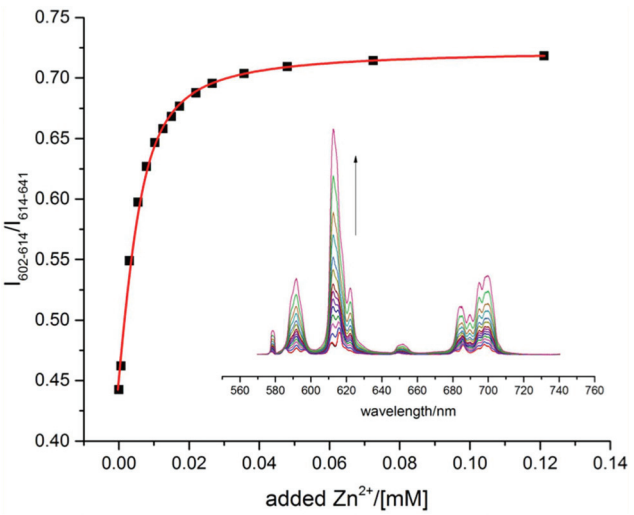

Fig. 6 Variation of the europium emission spectrum (inset) and the intensity ratio for [EuL^2] with added $ZnCl_2$, ([EuL^2] 8 μM, 0.1 M HEPES, pH = 7.40, 298 K, λ_{ex} = 335 nm). The binding constant (log K = 5.6) was fitted using a 1 : 1 binding model.

plexes can be regarded as useful emission probes for zinc ions in solution in this concentration regime, but in the absence of phosphate oxy-anions.

In the case of [EuL^1], a plausible binding mode (Scheme 5), involves coordination of six pyridine nitrogens, defining an octahedron around the zinc ion. The two tertiary nitrogen centres are further away from the Zn^{2+} ion, and do not participate in binding. A similar octahedral coordination of a zinc ion coordinated by two dipicolylamine moieties has been reported previously with a Zn^{2+} complex bearing a 'BTPA' ligand (Scheme 6).[33] However, in that structure the high steric demand encouraged the two tertiary nitrogen atoms to bind to the zinc atom, leaving two picolyl arms unbound. In contrast to [EuL^1], a tetrahedral configuration can be proposed for [EuL^2], involving two picolyl nitrogens, a tertiary amine nitrogen atom and one or two bound water molecules (Scheme 6), in line with the dominant 1 : 1 binding stoichiometry evidenced by the Job plot.

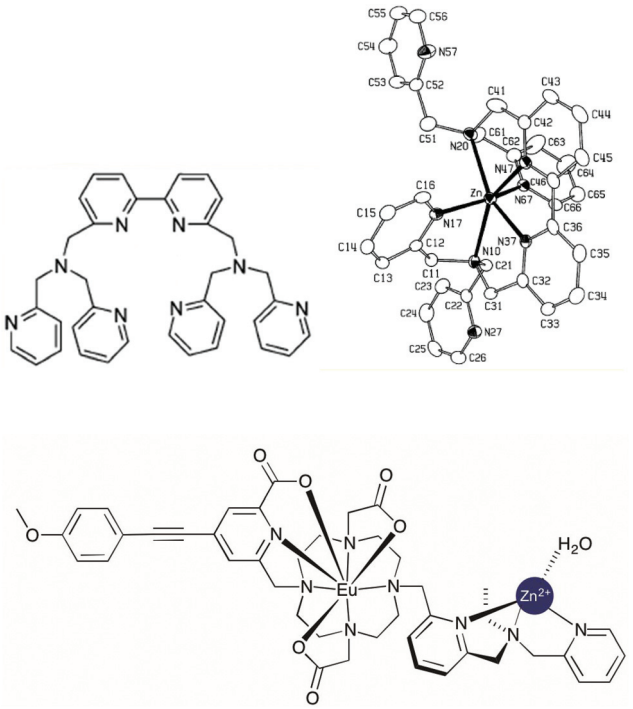

Scheme 6 (Upper) Molecular structure of the 'BTPA' ligand and its complex with Zn^{2+}.[33] and (lower) a possible binding motif for Zn^{2+} in its complex with [EuL^2], showing 1 : 1 complexation (other ligands or a water molecule may be bound to the zinc ion, including a bridging carboxylate oxygen of the nearby macrocyclic moiety).

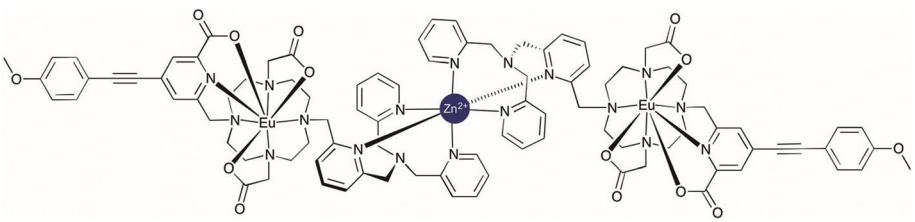

Scheme 5 Putative binding of Zn^{2+} with [EuL^1], in the 1 : 2 complex involving a bridging motif created by dissociation of one pyridine N atom from Eu.

With [Eu·L^1], values for the binding affinity of glyphosate were recorded in the presence of both one and two equivalents of added zinc salt (as $ZnCl_2$). For a 1 : 1 association model, values of log *K*, of 5.31 and 5.33 (±0.04) were found. These are the same values, within error, as those measured in the absence of added zinc ions, showing that the presence of the zinc salt in the mixture does not enhance overall affinity for glyphosate. A similar lack of sensitivity in the overall glyphosate response to the presence of added zinc ions was found with each of the other three complexes studied. Therefore, subsequent studies in more challenging background media were undertaken in the absence of added zinc salt, in each case.

Complexation behaviour in competitive media

A comparative study was undertaken to evaluate the ability of the four Eu(III) complexes to detect glyphosate in different background media, maintained at constant ionic strength (*I* = 0.1, NaCl) and buffered to pH 5.9. A one litre sample of water from the river Wear at Durham was taken in January 2017, during a period of normal flow. In order to sample levels of glyphosate in wheat and oat grains, sets of grains were soaked overnight in water and the filtrate was used as a background medium. The complexes [Eu·L^1] and [Eu·L^4] showed the most promising behaviour (Table 3), with good selectivity over the primary metabolite, AMPA. The former complex showed the largest spectral response in each case, with the overall intensity of emission increasing on glyphosate addition. It was selected for further study in wheat extracts, where the grain samples were 'spiked' with known concentrations of glyphosate, prior to analysis; the results of the Eu emission analyses were then compared to the known values.

The wheat grains were 'spiked' using stock solutions of glyphosate that had been diluted down to the appropriate concentration levels. Ten grains were selected, to which 0.01 mL of a glyphosate solution was added and left for 24 h in a closed system. The grains absorbed the glyphosate infused water, and the grains were subsequently freeze-dried and soaked for 24 h. The water was removed by lyophilisation and remade to a standard 2 mL volume, in a solution of complex of known concentration in 0.1 M MES/0.1 M NaCl solution. A stock solution of the complex was made up for these experiments, to minimise the risk that differences could arise from small fluctuations in complex concentration.

After an initial emission spectrum was measured, further increments of a standard solution of glyphosate were added to the complex solution, and the emission intensity ratio recorded. The variation in emission intensity ratio was plotted and compared to the calibration curve that had been derived earlier in simple aqueous wheat grain extract (Fig. 4).

Over the range from zero to 60 micromolar added glyphosate, there is a pseudo-linear section with a 35% modulation of the intensity ratio that could be regarded as a 'working' calibration curve. For the four series of samples, the use of the original calibration curve gave 84% recovery at 60 μM, 132% at 30 μM, 102% at 15 μM and 54% at 7.5 μM known glyphosate concentrations. The data points in Fig. 7 mostly lie above the

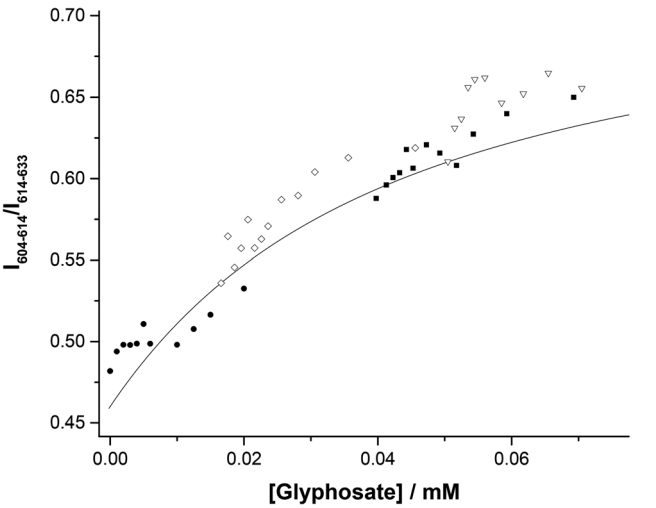

Fig. 7 Comparison of the calibration curve (line) for [Eu·L^1](7 μM, 0.1 M NaCl, 0.1 M MES, 295 K, pH 5.9, λ_{exc} 365 nm) with the data points derived from addition of increasing glyphosate concentrations between 0–0.06 mM, to the 'spiked grain' extracts for different initial glyphosate concentrations: 60 μM (triangles), 30 μM (squares), 15 μM (diamonds), 7.5 μM (circles).

Table 3 The estimated values of binding constants, as log *K* values for each complex with the stated analytes in aqueous buffer and for glyphosate only in a range of background media (295 K, pH 5.9, 0.1 M NaCl, 0.1 M MES)[a,e]

	Glyphosate					
Complex	Purite water	River water[d]	Oat extract	Grain extract	$H_2PO_4^-$	AMPA, **2**
[Eu·L^1]	5.36 (02)	4.92 (03)	4.77 (01)	4.42 (02)	4.35 (01)	3.30 (01)
[Eu·L^2]	3.11 (01)	3.07(02)	3.18 (0.01)	3.11 (0.01)	[b]	3.35 (02)
[Eu·L^3]	3.16 (01)	3.07(02)	3.57 (0.04)	3.34 (0.01)	[b]	3.16 (01)
[Eu·L^4]	4.92 (01)	4.04 (01)	4.88 (02)	3.54 (01)	[c]	3.20 (01)

[a] Errors stated refer to the statistical fit. [b] Under these conditions, weak or ill-defined binding was observed. [c] No spectral response to phosphate observed. [d] Independent ion chromatography analysis of this river water sample (ESI) showed it contained: 23.3 mM chloride, 9.91 mM sulphate, 0.87 mM nitrate, 0.70 mM fluoride and 0.01 mM phosphate; no glyphosate was detected and the water was filtered though 0.1 μ filters prior to use. The relatively high fluoride value reflects the mineral composition of Upper Weardale, where Fluorspar (CaF_2) is relatively abundant. [e] The measured binding constants for [Eu·L^1] with *N*-methylglyphosate, **3**, and the glyphosate metabolite aminomethylphosphonate, AMPA, **2**, were log *K* = 3.93 and 3.30 respectively.

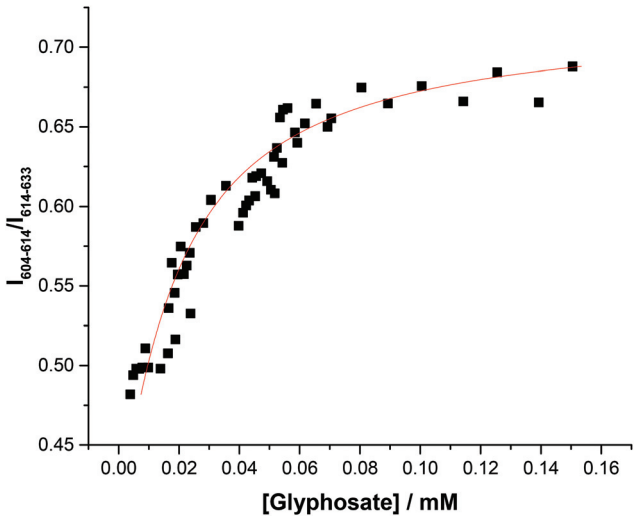

Fig. 8 Variation of the Eu emission intensity ratio as a function of glyphosate concentration combining the 'spiked grains' data sets, showing the best fit (line), associated with an apparent log *K* value of 4.97.

'calibration curve' determined in grain extract separately. Therefore, the 'spiked grain' data was fitted using non-linear least squares regression analysis, to calculate an apparent binding constant, for this common set of wheat grain extract data (Fig. 8).

Although there is some scatter, a binding curve was fitted to this large set of data to give an apparent log *K* value of 4.97 (±0.02), higher than the value found using the original calibration curve (log *K* = 4.42 (±0.02)). Such behaviour suggests that the complex binds to glyphosate in this aqueous grain extract slightly more strongly than originally surmised.

Because of the difference between the calibration curve originally calculated, and that found using the 'spiked grain' data, these experiments suggest that there may be some source of error in the readings that needs to be addressed. A reasonable explanation for the overall behaviour is that grain extract is a rather complex medium. Each grain may vary in concentrations of certain unknown species that can bind to the complex, or interact with it in some way. For example, how close the grain is to germination could affect the concentration of a number of different compounds. Future work therefore needs to use larger data sets and pay due respect to the need to calibrate the binding curve carefully.

Summary and conclusions

A series of four europium(III) complexes was synthesised, based on [Eu·L[1]] that had previously been shown to detect ATP and ADP. The tripicolylamino moiety was shown to be a critical structural feature in binding, as any alteration of it resulted in lower affinities. However, the exchange of the non-chromophoric pyridine group for a triazole moiety, *i.e.* [Eu·L[4]], resulted in a complex that did not bind to phosphate at 5.9 and responded more quickly to changes in analyte concentration.

Overall, the complex [Eu·L[1]] was found to behave best in binding glyphosate selectively in a range of different media. It acts as a 'switch-on' sensor, for which a number of emission intensity ratios can be used to track the binding to glyphosate and its congeners, operating over the range 5 to 50 μM.

Conflicts of interest

The authors declare no conflicts of interest.

Acknowledgements

We thank FScan Ltd for support, and Professor Robert Edwards and Dr Lami Nnamonu (Newcastle University) for samples of wheat grains. Robert Pal thanks the Royal Society for a University Research Fellowship.

Notes and references

1 J. Franz, *US Patent*, US3799758A, 1974. https://www.google.co.uk/patents/US3799758?dq=glyphosate+1974.
2 C. M. Benbrook, *Environ. Sci. Eur.*, 2016, **28**, 3.
3 D. M. Shah, S.G. Rogers, R. B. Horsch and R. T. Fraley, *US Patent*, US4940835, 1990.
4 S. Thongprakaisang, A. Thiantanawat, N. Rangkadilok, T. Suriyo and J. Satayavivad, *Food Chem. Toxicol.*, 2013, **59**, 126; International Agency for Research on Cancer Monographs – 112 Glyphosate, http://monographs.iarc.fr/ENG/Monographs/vol112/mono112-02.pdf, (accessed 5 February 2016); The IARC (International Agency for Research on Cancer) in 2015 labelled glyphosate as potentially carcinogenic to humans. In the same year, the EFSA (European Food Safety Authority) found that it was 'unlikely to pose any carcinogenic hazard to humans'. Due to these opposing views, the EU supported an independent study by the European Chemicals Agency (ECHA). In June 2017, they declared that there was insufficient evidence to classify glyphosate as carcinogenic. Widespread concern over the herbicide has led to the temporary renewal period being five years rather than the standard fifteen, by the European Commission. Its use was banned in California in July 2017, as the state proclaimed that the herbicide is carcinogenic.
5 M. Boocock and J. R. Coggins, *FEBS Lett.*, 1983, **154**, 127–133.
6 J. M. Becerril, S. O. Duke and J. Lydon, *Phytochemistry*, 1989, **28**, 695–699.
7 E. G. Jaworski, *J. Agric. Food Chem.*, 1972, **20**, 1195–1198.
8 National Primary Drinking Water Regulations, https://www.epa.gov/ground-water-and-drinking-water/national-primary-drinking-water-regulations.

9 S. Brosillon, D. Wolbert, M. Lemasle, P. Roche and A. Mehrsheikh, *Water Res.*, 2006, **40**, 2113–2124.
10 Joint FAO/WHO meeting on pesticide residues, http://www.who.int/foodsafety/call4data_2017JMPR.pdf, 15.EU, 2016: http://ec.europa.eu/food/plant/pesticides/eu-pesticides-database/public/?event=activesubstance.selection&language=EN.
11 EU pesticide database, http://ec.europa.eu/food/plant/pesticides/eu-pesticides-database/public/?event=activesubstance.selection&language=EN.
12 Agricultural and Veterinary Chemicals Code Instrument No. 4 (MRL Standard)2012, https://www.legislation.gov.au/Details/F2017C00649.
13 Code of Federal Regulations, https://www.gpo.gov/fdsys/pkg/CFR-2014-title40-vol24/xml/CFR-2014-title40-vol24-part180.xml.
14 J. Pouessel, S. Abada, N. Le Bris, M. Elhabiri, L. C. Charbonnière and R. Tripier, *Dalton Trans.*, 2013, **42**, 4859–4872.
15 Y. Liu and M. Bonizzoni, *J. Am. Chem. Soc.*, 2014, **136**, 14223–14229.
16 T. Minami, Y. Liu, A. Akdeniz, P. Koutnik, N. A. Esipenko, R. Nishiyabu, Y. Kubo and P. Anzenbacher, *J. Am. Chem. Soc.*, 2014, **136**, 11396–11401.
17 E. R. Neil and D. Parker, *RSC Adv.*, 2017, **7**, 4531–4540; B. K. McMahon and D. Parker, *RSC Adv.*, 2014, **4**, 37649–37654; S. J. Butler, B. K. McMahon, R. Pal, J. W. Walton and D. Parker, *Chem. – Eur. J.*, 2013, **19**, 9511–9517; D. G. Smith, R. Pal and D. Parker, *Chem. – Eur. J.*, 2012, **18**, 11604–11613; R. Pal, L. C. Costello and D. Parker, *Org. Biomol. Chem.*, 2009, **7**, 1525–1528.
18 For selected reviews on anion recognition in water with lanthanide systems: J.-C. G. Bünzli, *Chem. Rev.*, 2010, **110**, 2729–2755; M. C. Heffern, L. M. Matosziuk and T. J. Meade, *Chem. Rev.*, 2014, **114**, 4496–4539; S. J. Butler and D. Parker, *Chem. Soc. Rev.*, 2013, **42**, 1652–1666; S. Shuvaev, M. Starck and D. Parker, *Chem. – Eur. J.*, 2017, **23**, 9974–9989. For selected examples of the signalling of organophosphate species in solution: R. Mailhot, T. Traviss-Pollard, R. Pal and S. J. Butler, *Chem. – Eur. J.*, 2018, **24**, 10745–10755; S. H. Hewitt, J. Parris, R. Mailhot and S. J. Butler, *Chem. Commun.*, 2017, **53**, 12626–12629; M. Wang, H. Ye, L. You and X. Chen, *ACS Appl. Mater. Interfaces*, 2016, **8**, 574–581.
19 E. R. Neil, M. A. Fox, R. Pal and D. Parker, *Dalton Trans.*, 2016, **45**, 8355–8366.
20 S. Shuvaev, M. A. Fox and D. Parker, *Angew. Chem., Int. Ed.*, 2018, **57**, 7488–7492.
21 T. G. Appleton, J. R. Hall and I. J. McMahon, *Inorg. Chem.*, 1986, **25**, 726–734; R. J. Motekaitis and A. E. Martell, *J. Coord. Chem.*, 1985, **14**, 139–149.
22 M. Peixoto, G. F. Bauerfeldt, M. H. Herbst, M. S. Pereira and C. O. da Silva, *J. Phys. Chem. A*, 2015, **119**, 5241–5249.
23 K. Mason, A. C. Harnden, C. W. Patrick, A. W. J. Poh, A. S. Batsanov, E. A. Suturina, M. Vonci, E. J. L. McInnes, N. F. Chilton and D. Parker, *Chem. Commun.*, 2018, **54**, 8486–8489.
24 O. A. Blackburn, R. M. Edkins, S. Faulkner, A. M. Kenwright, N. J. Rogers, S. Shuvaev and D. Parker, *Dalton Trans.*, 2016, **45**, 6782–6800.
25 G. Anderegg and F. Wenk, *Helv. Chim. Acta*, 1967, **50**, 2330–2332.
26 (*a*) A. D. Becke, *J. Chem. Phys.*, 1993, **98**, 5648–5652; (*b*) C. Lee, W. Yang and R. G. Parr, *Phys. Rev. B: Condens. Matter Mater. Phys.*, 1988, **37**, 785–789.
27 (*a*) J. S. Binkley, J. A. Pople and W. J. Hehre, *J. Am. Chem. Soc.*, 1980, **102**, 939–947; (*b*) M. S. Gordon, J. S. Binkley, J. A. Pople, W. J. Pietro and W. J. Hehre, *J. Am. Chem. Soc.*, 1982, **104**, 2797–2803; (*c*) W. J. Pietro, M. M. Francl, W. J. Hehre, D. J. Defrees, J. A. Pople and J. S. Binkley, *J. Am. Chem. Soc.*, 1982, **104**, 5039–5048; (*d*) K. D. Dobbs and W. J. Hehre, *J. Comput. Chem.*, 1986, **7**, 359–378; (*e*) K. D. Dobbs and W. J. Hehre, *J. Comput. Chem.*, 1987, **8**, 861–879; (*f*) K. D. Dobbs and W. J. Hehre, *J. Comput. Chem.*, 1987, **8**, 880–893.
28 M. J. Frisch, G. W. Trucks, H. B. Schlegel, G. E. Scuseria, M. A. Robb, J. R. Cheeseman, G. Scalmani, V. Barone, B. Mennucci, G. A. Petersson, H. Nakatsuji, M. Caricato, X. Li, H. P. Hratchian, A. F. Izmaylov, J. Bloino, G. Zheng, J. L. Sonnenberg, M. Hada, M. Ehara, K. Toyota, R. Fukuda, J. Hasegawa, M. Ishida, T. Nakajima, Y. Honda, O. Kitao, H. Nakai, T. Vreven Jr., J. A. Montgomery, J. E. Peralta, F. Ogliaro, M. Bearpark, J. J. Heyd, E. Brothers, K. N. Kudin, V. N. Staroverov, R. Kobayashi, J. Normand, K. Raghavachari, A. Rendell, J. C. Burant, S. S. Iyengar, J. Tomasi, M. Cossi, N. Rega, J. M. Millam, M. Klene, J. E. Knox, J. B. Cross, V. Bakken, C. Adamo, J. Jaramillo, R. Gomperts, R. E. Stratmann, O. Yazyev, A. J. Austin, R. Cammi, C. Pomelli, J. W. Ochterski, R. L. Martin, K. Morokuma, V. G. Zakrzewski, G. A. Voth, P. Salvador, J. J. Dannenberg, S. Dapprich, A. D. Daniels, O. Farkas, J. B. Foresman, J. V. Ortiz, J. Cioslowski and D. J. Fox, *Gaussian 09, Revision A.02*, Gaussian, Inc., Wallingford CT, 2009.
29 (*a*) M. Soulié, F. Latzko, E. Bourrier, V. Placide, S. J. Butler, R. Pal, J. W. Walton, P. L. Baldeck, B. Le Guennic, C. Andraud, J. M. Zwier, L. Lamarque, D. Parker and O. Maury, *Chem. – Eur. J.*, 2014, **20**, 8636–8646; (*b*) T. T. da Cunha, J. Jung, M.-E. Boulon, G. Campo, F. Pointillart, C. L. M. Pereira, B. Le Guennic, O. Cador, K. Bernot, F. Pineider, S. Golhen and L. Ouahab, *J. Am. Chem. Soc.*, 2013, **135**, 16332–16335; (*c*) K. Sénéchal-David, A. Hemeryck, N. Tancrez, L. Toupet, J. A. G. Williams, I. Ledoux, J. Zyss, A. Boucekkine, J.-P. Guégan, H. Le Bozec and O. Maury, *J. Am. Chem. Soc.*, 2006, **128**, 12243–12255; (*d*) F. Pointillart, B. Le Guennic, O. Maury, S. Golhen, O. Cador and L. Ouahab, *Inorg. Chem.*, 2013, **52**, 1398–1408.
30 J. Tomasi, B. Mennucci and E. Cancès, *J. Mol. Struct. (Theochem)*, 1999, **464**, 211–226.

31 C. F. Macrae, I. J. Bruno, J. A. Chisholm, P. R. Edgington, P. McCabe, E. Pidcock, L. Rodriguez-Monge, R. Taylor, J. van de Streek and P. A. Wood, *J. Appl. Crystallogr.*, 2008, **41**, 466–470.
32 A. Beeby, I. M. Clarkson, R. S. Dickins, S. Faulkner, D. Parker, L. Royle, A. S. de Sousa, J. A. G. Williams and M. Woods, *J. Chem. Soc., Perkin Trans. 2*, 1999, 493–503.
33 C. Brady, P. L. Callaghan, Z. Ciunik, C. G. Coates, A. Døssing, A. Hazell, J. J. McGarvey, S. Schenker, H. Toftlund, A. X. Trautwein, H. Winkler and J. A. Wolny, *Inorg. Chem.*, 2004, **43**, 4289–99.